

# Metronomic photodynamic therapy for deep organ cancer by implantable wireless OLEDs

Cite as: APL Bioeng. 9, 026113 (2025); doi: [10.1063/5.0256898](https://doi.org/10.1063/5.0256898)

Submitted: 7 January 2025 · Accepted: 13 April 2025 ·

Published Online: 30 April 2025










View Online



Export Citation



CrossMark

Yujiro Itazaki,<sup>1</sup>  Kei Sakanoue,<sup>2</sup> Katsuhiko Fujita,<sup>3</sup>  Izumi Kirino,<sup>4</sup> Kazuhiro Eguchi,<sup>2</sup> Yutaka Miyazono,<sup>2</sup> Ryoichi Yamaguchi,<sup>5</sup> Takasumi Tsunenari,<sup>1</sup>  Takao Sugihara,<sup>1</sup> Kenji Kuwada,<sup>6</sup> Naoki Kobayashi,<sup>6</sup> Tsuyoshi Goya,<sup>6</sup>  Katsuyuki Morii,<sup>6,7</sup>  Hironori Tsujimoto,<sup>1</sup>  and Yuji Morimoto<sup>8,a)</sup> 

## AFFILIATIONS

<sup>1</sup>Department of Surgery, National Defense Medical College, Saitama, Japan

<sup>2</sup>Pleiades Technologies LLC., Fukuoka, Japan

<sup>3</sup>Institute for Materials Chemistry and Engineering, Kyushu University, Fukuoka, Japan

<sup>4</sup>Division of Hepato-Biliary-Pancreatic Surgery and Transplantation, Department of Surgery, Graduate School of Medicine, Kyoto University, Kyoto, Japan

<sup>5</sup>Kumamoto Industrial Research Institute, Kumamoto, Japan

<sup>6</sup>NIPPON SHOKUBAI CO., LTD., Osaka, Japan

<sup>7</sup>Nippon Shokubai Research Alliance Laboratories, Osaka University, Osaka, Japan

<sup>8</sup>Department of Physiology, National Defense Medical College, Saitama, Japan

<sup>a)</sup> Author to whom correspondence should be addressed: [moyan@ndmc.ac.jp](mailto:moyan@ndmc.ac.jp)

## ABSTRACT

Metronomic photodynamic therapy (mPDT) is a method of continuously delivering low-intensity light to a cancer lesion. This approach does not require high-intensity light, enabling the miniaturization of light devices and making them suitable for implantation within the body. However, the application of mPDT to tumors in deep organs such as the liver and pancreas has yet to reach practical implementation. In this study, we developed an mPDT system designed to meet three key requirements deemed essential for practical use: (1) uniform light irradiation throughout the tumor, (2) maintenance of constant light intensity within the body with sufficient operational duration, and (3) avoidance of immunological complications and thermal damage. The newly constructed mPDT system incorporates an ultra-thin organic light-emitting diode (OLED) device and wireless energy transfer technology, allowing it to be designed for implantation in deep organs. In experiments using a rat model of orthotopic hepatoma, the new mPDT system effectively induced widespread cell death deep within the tumor and exhibited high therapeutic efficacy against cancer. This study is the first study to demonstrate that mPDT utilizing a biocompatible and wirelessly powered OLED device has strong anti-tumor effects against parenchymal organ cancers. The findings represent a significant advancement toward the clinical application of mPDT for the treatment of deep organ cancers.

© 2025 Author(s). All article content, except where otherwise noted, is licensed under a Creative Commons Attribution-NonCommercial 4.0 International (CC BY-NC) license (<https://creativecommons.org/licenses/by-nc/4.0/>). <https://doi.org/10.1063/5.0256898>

## INTRODUCTION

Photodynamic therapy (PDT) uses photosensitizer (PS) activation by intense, brief light exposure ( $>100 \text{ mW/cm}^2$  for  $\sim 10 \text{ min}$ ) to generate reactive oxygen species, resulting in the death of cancer cells.<sup>1</sup> PDT is clinically approved for the treatment of superficial cancers in organs such as the esophagus, lung, stomach, cervix, and brain. Tumors can be irradiated directly by a light source or through an optical fiber.

Metronomic PDT (mPDT) is a newly developed method using repeated PS administration with continuous low-intensity light.<sup>2</sup> Unlike conventional PDT with light intensity of more than  $100 \text{ mW/cm}^2$ , mPDT uses less than  $1 \text{ mW/cm}^2$  of light intensity. This reduces thermal damage risks and allows the light source to be miniaturized and implanted in the body.<sup>3</sup> In addition, extended illuminating time (several days) in mPDT can continuously inhibit tumor growth. The authors previously developed a wirelessly

powered LED device for mPDT and proved its efficacy against subcutaneous tumors.<sup>4,5</sup>

Despite promising developments, mPDT using implantable devices for tumors in deep organs, such as the liver and pancreas, has not yet reached practical application. To address this gap, the authors have constructed an mPDT system for deep organs that meets three key requirements considered necessary for practical use: (1) the ability to uniformly deliver light to the entire tumor area,<sup>6</sup> (2) unchanging light intensity and sufficient operational duration<sup>7</sup> maintained within the body, and (3) avoidance of immunological complications<sup>8</sup> or thermal damage.<sup>9</sup>

A novel mPDT system that is the first to successfully achieve deep organ cancer regression using an implantable, ultra-thin organic light-emitting diode (OLED) device with wireless power transmission is presented in this report. Unlike previous LED-based mPDT systems, the OLED technology enables more uniform light distribution, higher biocompatibility, and flexible implantation anywhere in the body. This addresses critical limitations in deep organ mPDT, for which achieving consistent and prolonged light exposure has been a major barrier to clinical translation.

To validate the feasibility and efficacy of this system, we conducted experiments in a rat model of orthotopic hepatoma, and the results showed significant tumor regression. Our findings highlight the robust anti-tumor effects of OLED-based mPDT for parenchymal organ cancers, marking a key step toward clinical application. This study represents a breakthrough in deep organ cancer treatment by overcoming the limitations of existing mPDT systems and paving the way for practical, implantable light-based therapies.

## RESULTS

A conceptual diagram of mPDT using the new device is shown in Fig. 1. The implantable wirelessly driven OLED device is placed on the tumor surface of the deep organ. The tumor is continuously illuminated by the OLED with repeated administration of the PS.

### Wirelessly powered OLED device and power transmission platform

The implantable OLED device measures  $15.0 \times 16.0 \times 1.8$  mm, weighs 0.6 g, and features a circular 8-mm emitting area covering the cancer lesion [Figs. 2(a) and 2(b)]. Its structure includes multiple functional layers on a 50- $\mu$ m-thick polyethylene terephthalate substrate, with added components for wireless power: a 13.6-mm diameter coil tuned to 13.56 MHz, a matching circuit, and a ferrite sheet for electromagnetic shielding [Fig. 2(c), [supplementary material Table 1](#)]. The OLED achieves uniform luminescence ( $\pm 0.8\%$  variation) and high linearity of luminance to operating power (correlation  $> 0.979$ ) [[supplementary material Figs. 1\(a\) and 1\(b\)](#)]. Both green ( $\sim 540$  nm) and red ( $\sim 620$  nm) OLEDs perform consistently, efficiently exciting temoporfin (mTHPC),<sup>10</sup> a PS, due to overlapping emission and absorption spectra [[supplementary material Fig. 1\(c\)](#)]. The device is coated with UV-curing resin and Parylene C<sup>11</sup> for waterproofing and biocompatibility, ensuring durability and insulation ([supplementary material Figs. 2 and 3](#)).

In experiments using animals, mPDT requires stable, low-intensity, continuous illumination, even when animals are freely moving. To achieve this, a power transmission platform was constructed, using a

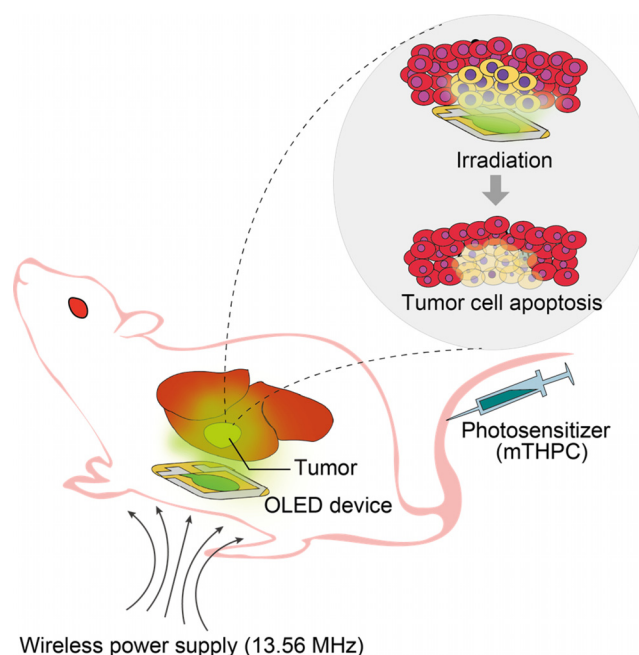


**FIG. 1.** Concept of mPDT using the OLED device. After the OLED device has been attached to the tumor in the animal, the OLED emits light by wireless power while the PS is repeatedly administered to the animal, inducing cell death in the tumor. mTHPC: temoporfin.

uniaxial Helmholtz coil antenna large enough to fit standard rodent cages [Fig. 2(d) and 2(e)]. This ensures uniform power, maintaining OLED irradiance at  $565 \pm 100 \mu\text{W}/\text{cm}^2$  with  $\pm 18\%$  variability regardless of the animal's posture ([supplementary material Fig. 4](#)).

### Metronomic PDT using the implantable OLED device

An orthotopic rat hepatoma model was established by inoculating N1S1 cancer cells<sup>12</sup> into subserous tissue of the left hepatic lobe. Four days after the inoculation, a PS (mTHPC) was administered intravenously (0.5 mg/kg). At that time point, the tumor size was 20–30 mm<sup>3</sup>. The OLED device was attached to the liver with adhesive drops at the corners of the device (four points) so that the emitting surface covered the tumor (Fig. 3).

The OLED device attached to the liver emitted light via a wireless power supply ([supplementary material Video 1](#)) and continued to emit light stably under conditions of body motion ([supplementary material Video 2](#)) after abdominal closure.

### Anti-tumor efficacy of mPDT using OLED devices and enhancement with repeated photosensitizer administration

An investigation was conducted to demonstrate the anti-tumor effects of mPDT using OLED devices. Following single administration of a photosensitizer (PS), low-intensity light averaging approximately  $570 \mu\text{W}/\text{cm}^2$  ([supplementary material Fig. 6](#)) was illuminated continuously for 4 days [Fig. 4(a), "Protocol 1 $\times$ PS"]. Tumor volume was assessed using ultrasound imaging based on measurements taken before

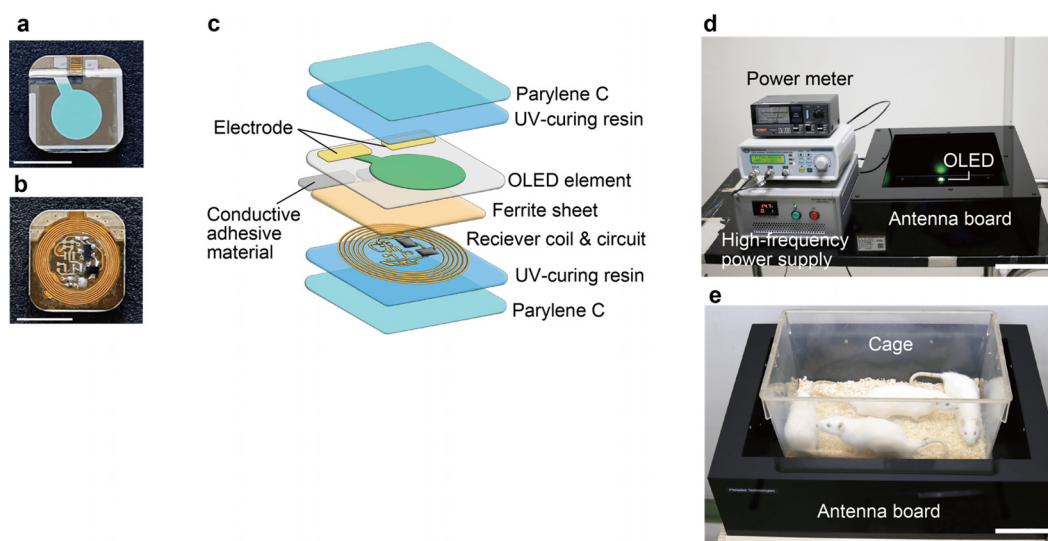


**FIG. 2.** Implantable OLED device (a–c) and power transmission platform system (d, e). The OLED element is housed on one side (a) and the power-receiving coil is on the opposite side (b). Scale bar = 10 mm. (c) Stratified structures of the OLED device. (d) Power transmission platform system. Scale bar = 100 mm. (e) Animals moving around in a cage on the antenna board. Scale bar = 100 mm.

and after treatment [Fig. 4(b)]. The findings revealed that tumor growth was significantly suppressed compared to that in the control group. Post-treatment tumor volume in the control group was  $263 \text{ mm}^3$  [Fig. 4(e), “Control”]. In the treatment group, post-treatment tumor volume was reduced to  $106 \text{ mm}^3$ , approximately 40% of the volume in the control group [Fig. 4(e), “Light (+)  $1 \times \text{PS}$ ”]. Additionally, mPDT induced whitening of tissues in contact with the OLED luminescent surface, and cross-sectional observations confirmed that the entire tumor lesion had turned white [Fig. 4(c), “Light (+)  $1 \times \text{PS}$ ”]. Histopathological images further revealed apoptotic changes in the regions exhibiting anti-tumor effects, with increases in nuclear abnormalities (pyknosis and karyorrhexis) and TUNEL-positive cells [Fig. 4(d), “Light (+)  $1 \times \text{PS}$ ”].

Since mPDT involves long-term light irradiation, the therapeutic effect may be further enhanced by repeated PS administration. To

explore this possibility, the impact of repeated PS administration on treatment efficacy was evaluated. When the PS was administered twice during the 4-day period of low-intensity light illumination [Fig. 4(a), “Protocol  $2 \times \text{PS}$ ”], suppression of tumor growth was greater than that in the case of single PS administration. After treatment, the tumor volume was reduced to  $38 \text{ mm}^3$  [Fig. 4(e), “Light (+)  $2 \times \text{PS}$ ”], corresponding to approximately 14% of the tumor volume in the control group. Furthermore, the two-dose protocol resulted in a broader area of cell death and a higher apoptosis fraction than those with single-dose mPDT [Fig. 4(f)]. Notably, the therapeutic effects extended to the tumor margins, where no residual tumor cells were detected, and only a sparse presence of tumor cells was observed at the deeper boundary regions [Fig. 4(d), “Light (+)  $2 \times \text{PS}$ ”].

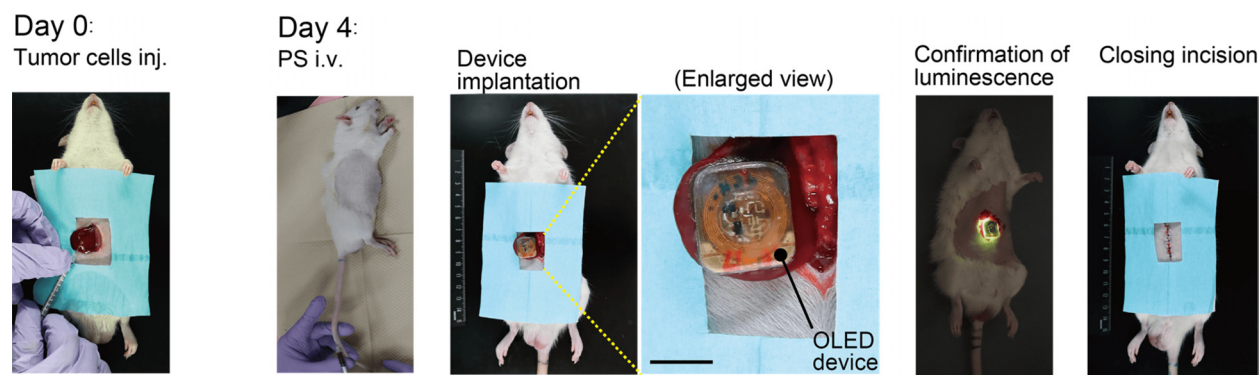


**FIG. 3.** Orthotopic rat hepatoma model and OLED device implantation. Sequential steps illustrating the construction of a hepatoma model in a rat. Day 0: Injection of tumor cell suspension into the hepatic lobe (Tumor cells inj.). Day 4: Intravenous administration of the photosensitizer via the tail vein (PS i.v.). This is followed by the surgical implantation of an OLED device (Device implantation) and confirmation of the device's luminescence (Confirmation of luminescence). The liver is returned to its original position with the OLED attached and then the skin wound is closed (Closing incision).



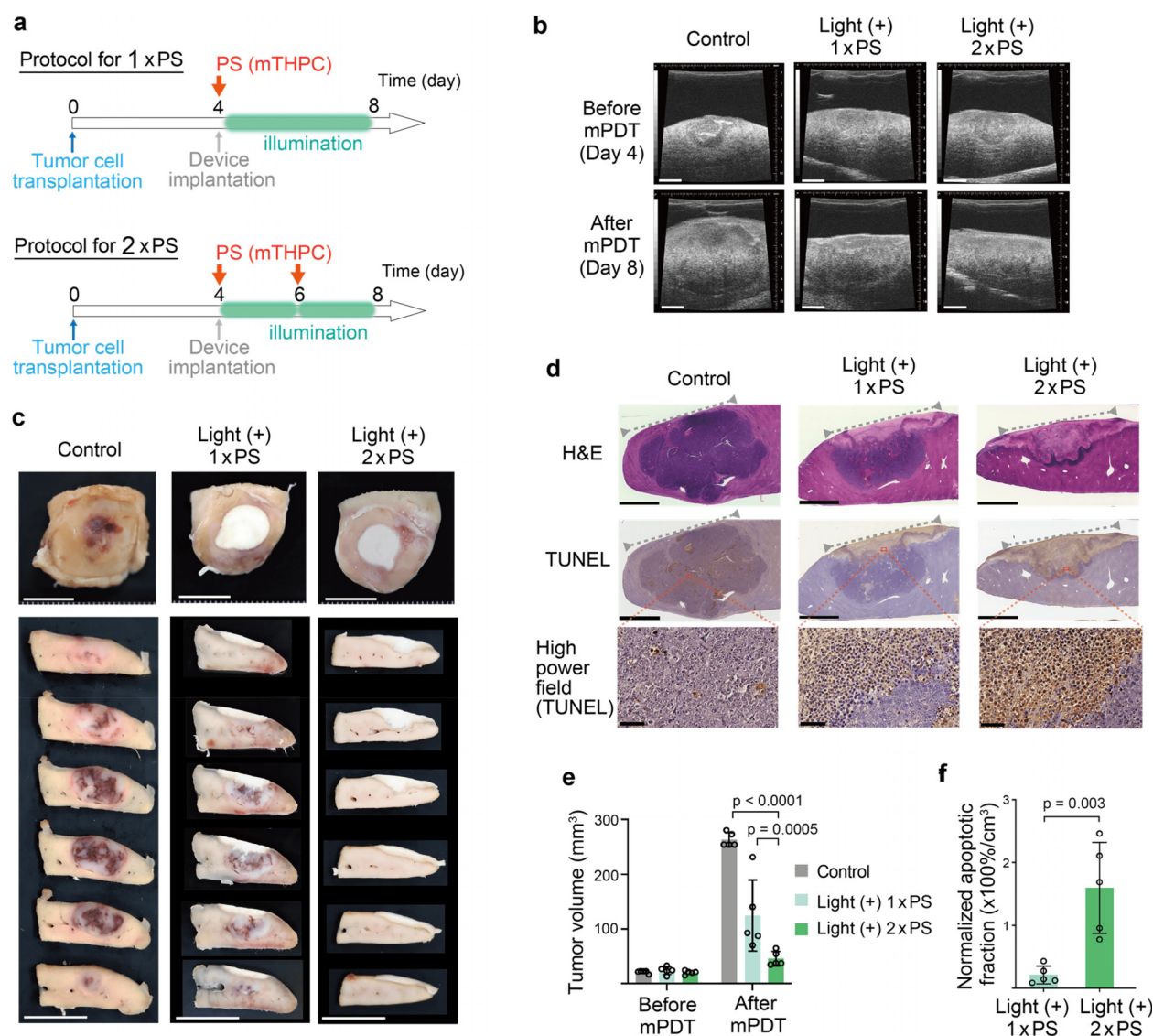


**FIG. 4.** Anti-tumor effects of mPDT using the OLED device and enhancement of the effects by repeated PS administration. (a) Experimental protocol for mPDT with change in the frequency of PS administration. Rats were inoculated with cancer cells in the liver lobe and the OLED device was implanted after an interval of 4 days. The PS was then administered via the caudal vein, and the tumor was illuminated for 2 days. In the protocol of one-time use of the PS, an additional 2 days of illumination was executed without additional administration of the PS, whereas in the protocol with two-time use of PSs, an additional 2 days of illumination was executed with additional administration of the PS. (b) Ultrasound images before and after mPDT. The echo value of the tumor tissue is slightly lower than that of the surrounding liver tissue, which allows detection of the tumor border. (c) Liver surface after removal of the OLED after mPDT (top panels) and cross-section of the liver specimen sliced at 2-mm intervals in the ventrodorsal direction (bottom panels). The mPDT-treated liver surface shows distinct pallor changes. (d) Cross-sectional views of tumors after mPDT: H&E staining (top panels), TUNEL staining (middle panels), and high magnification image of the TUNEL staining (bottom panels). Dashed lines with arrowheads on the tumor surface indicate the position of the OLED emitting surface. (e) Contrastive analysis of tumor volume changes in each experimental group before and after mPDT ( $n = 5$ , each). (f) Normalized apoptotic fractions, reflecting cell death relative to tumor volume ( $n = 5$ , each). Scale bars: 2 mm in (b), 10 mm in (c), 0.05 mm in high magnification and 2.5 mm in other histopathology images for (d). The transmitter power was set at 8 W. "Control": group with two doses of PS and a non-emitting device. "Light (+) 1xPS": group with one dose of PS and a light-emitting device. "Light (+) 2xPS": group with one PS dose, light illumination, and another PS dose during illumination.

These findings strongly indicate that repeated administration of a PS substantially enhances the therapeutic efficacy of mPDT.

### Illumination wavelengths and treatment efficacy

In conventional PDT, red light is commonly used due to its superior tissue penetration capabilities.<sup>13</sup> However, the influence of light

wavelength on the therapeutic efficacy of mPDT remains inadequately understood. Therefore, this study was conducted to investigate this relationship.

In order to determine the predominant OLED emission wavelength in tumor therapeutic efficacy, the following three experimental groups (all with the PS administered twice) were studied according to

the protocol shown in Fig. 5(a): (i) a group implanted with a green luminescent device, (ii) a group implanted with a red luminescent device, and (iii) a group with a non-emitting device (control).

Metronomic PDT with red OLEDs showed a significantly larger therapeutic area than that with mPDT using green OLEDs [Figs. 5(d) and 5(e)]. Specifically, the red OLEDs significantly increased the therapeutic effect in both vertical [Fig. 5(f)] and horizontal [Fig. 5(g)] directions based on the emitting area, especially in the horizontal direction across the emitting area [Figs. 5(e) and 5(g)]. As a result, mPDT with the red OLED induced more tumor cell death [Figs. 5(e) and 5(h)] and the tumor volume was significantly smaller than that when mPDT with the green OLED was used [Fig. 5(c)].

These findings indicate that, as with conventional PDT, red light enhances the therapeutic efficacy of metronomic PDT compared to that with green light.

### Evaluation of mPDT safety: Hepatic enzyme levels, histological effects, and foreign body response

To assess potential adverse effects, blood samples were collected before and after mPDT to measure hepatic enzymes. Aspartate aminotransferase (AST) and alanine aminotransferase (ALT) levels during treatment showed no significant difference between the two-time mPDT group and control group [supplementary material Figs. 7(a)

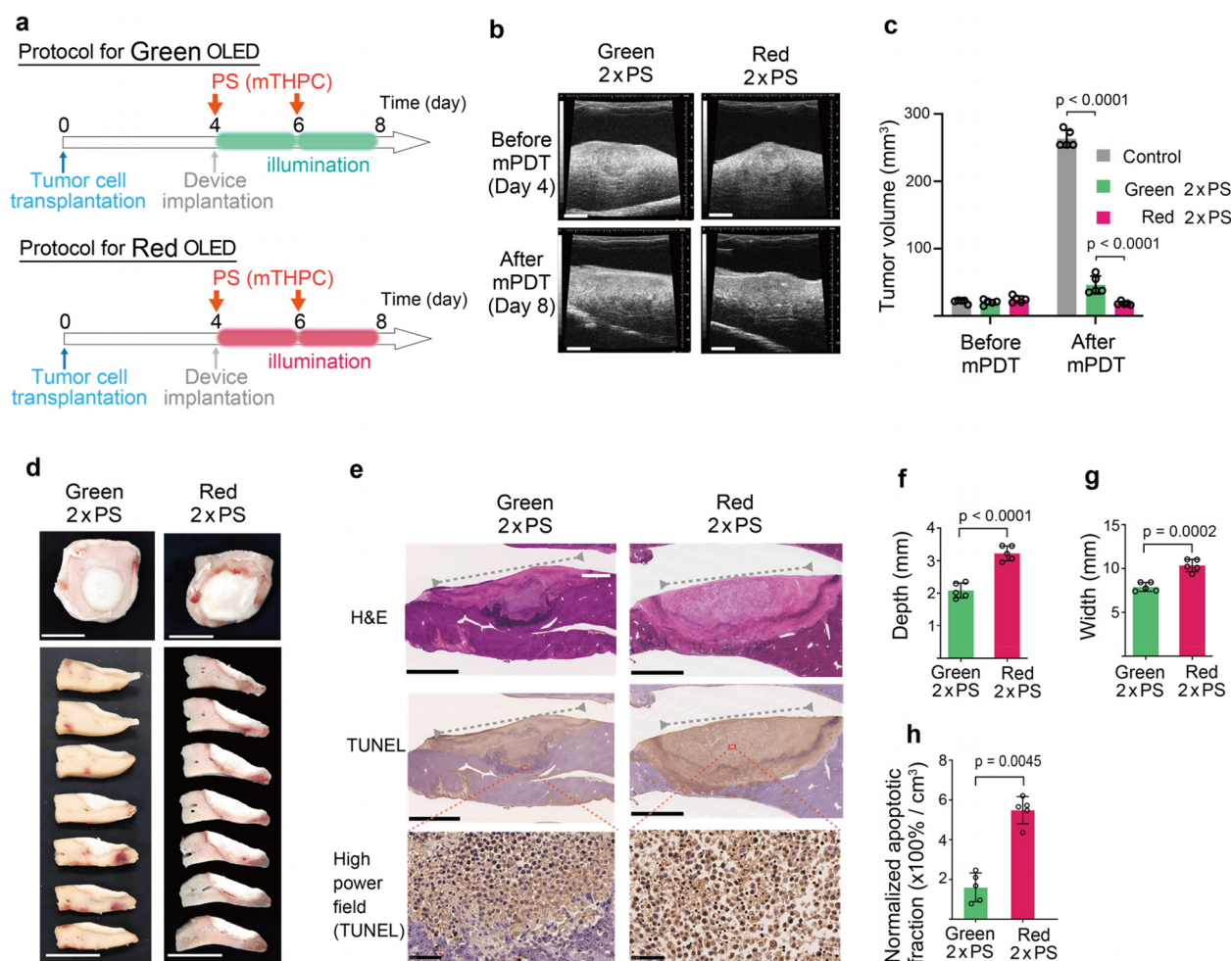


**FIG. 5.** Augmentation of anti-tumor effects with red OLEDs. (a) Experimental protocol for mPDT using OLED devices with different emission wavelengths: same procedure as that for "Protocol 2xPS" shown in Fig. 4(a) with only the emission wavelength of the device to be implanted being different. (b) Ultrasound images before and after mPDT. (c) Tumor volume changes in each experimental group before and after mPDT ( $n=5$ , each). (d) Liver surface after removal of the OLED after mPDT (top panels) and cross-section of the liver specimen sliced at 2-mm intervals in the ventrodorsal direction (bottom panels). The mPDT-treated liver surface shows distinct pallor changes. (e) Cross-sectional views of tumors after mPDT: H&E staining (top panels), TUNEL staining (middle panels), and high magnification image of the TUNEL staining (bottom panels). Dashed lines with arrowheads on the tumor surface indicate the position of the OLED emitting surface. (f) Deepest reach of the cell death zone in the vertical direction of the emission plane. (g) Maximum reach of the cell death zone in the horizontal direction of the emitting plane. (h) Normalized apoptotic fractions, reflecting cell death relative to tumor volume ( $n=5$ , each). Scale bars: 2 mm in (b), 10 mm in (d), 0.05 mm in high magnification and 2.5 mm in other histopathology images for (e). The transmitter power was set at 8 W for both green and red OLEDs. "Control": group with two doses of PS and a non-emitting device. "Green 2xPS": group with one PS dose, green OLED activation, and another PS dose during illumination. "Red 2xPS": group with one PS dose, red OLED activation, and another PS dose during illumination.

and 7(b)]. Similarly, changes in body weight over time during treatment were not significantly different between the groups [supplementary material Fig. 7(c)].

Histological analysis revealed that mPDT-induced cell death not only in tumor cells but also in normal hepatocytes within the tumor margin [Figs. 4(d) and 5(e)]. However, this peritumoral hepatocyte cell death is likely to contribute to tumor regression, as previous studies suggested that disruption of the tumor-supporting microenvironment can enhance treatment efficacy.<sup>14,15</sup> These findings indicate that while mPDT affects the peritumoral region, it does not cause significant systemic toxicity or further hepatic damage, as reflected in stable AST and ALT levels.

On the emitting side of the OLED device in contact with the liver, the parylene coating effectively suppressed fibrous tissue formation, which can be induced by a foreign body reaction, compared to that in the non-coated condition, enabling a reduction in its thickness to approximately 100  $\mu\text{m}$  [supplementary material Figs. 3(a) and 3(b)]. In contrast, on the non-contact side of the device, a fibrous tissue layer of approximately 1 mm in thickness was observed [supplementary material Fig. 3(c)], presumably due to an enhanced foreign body response triggered by exposure to intra-body cavity fluid flow. However, since this is the non-emitting side with no functional impact, and given that some degree of fibrous tissue formation is inevitable in medical device implantation, it poses no practical concerns.

## DISCUSSION

To realize mPDT for deep organ cancer, a thin, lightweight, biocompatible, and wirelessly powered OLED device that can cover the tumor surface and illuminate the entire tumor has been newly constructed. Using this device, mPDT successfully reduced tumor size in an orthotopic rat hepatoma model.

The use of the OLED device has made it possible to distribute light homogeneously and to cover the marginal boundaries of the tumor. This effectively activates localized PSs and produces massive anti-tumor effects. Since tumors grow by replacing adjacent healthy tissue,<sup>16</sup> illuminating the tumor margin is crucial. Including the surrounding healthy tissue in the illumination helps reduce tumor regrowth.<sup>14,15</sup>

The OLED device constructed in this study was coated with Parylene C not only for waterproofing<sup>17</sup> but also for biocompatibility,<sup>18</sup> and it was shown to have sufficient immunological biosafety for remaining in the body long enough for deep organ cancer treatment. Since the rise in temperature during treatment was only 1 °C at most, thermal damage to the normal tissue surrounding the tumor, which is a concern when using stronger light such as laser,<sup>19</sup> was not observed.

The spread of cancer cells through surgical incisions and punctures of the tumors, one of the major concerns in cancer treatment,<sup>20</sup> can be minimized because the OLED device is simply attached and fixed to the surface of the tumor. This device maintains a more stable position relative to the lesion than conventional endoscopic methods, as it ensures consistent alignment between the light source and the tumor, resulting in a more stable and effective light delivery directly to the tumor. Therefore, therapeutic effects can be expected in long-term treatment.

Metronomic PDT with administration of the PS twice efficiently disintegrated tumor cells, leading to tumor tissue shrinkage. On the other hand, even in conventional PDT, repeated PDT has been shown

to enhance the anti-tumor effect.<sup>21</sup> These findings suggest that as apoptotic tumor cells at the surface shrink, light penetration improves, allowing deeper layers of the tumor to be exposed to effective irradiation. Additionally, the photosensitizer that accumulated in viable tumor cells beneath the apoptotic and shrunken layers is expected to react with the extended light exposure, potentially further enhancing the anti-tumor effect in deeper regions.

Furthermore, fluorescence imaging at high magnification [supplementary material Fig. 8(a)] revealed that the distribution of the photosensitizer within the tumor tissue does not always coincide with perivascular regions. This suggests that, in addition to vascular transport, alternative pathways such as infiltration of phagocytic cells, including macrophages, from the surrounding tumor microenvironment may facilitate photosensitizer delivery into the tumor at a cellular level.<sup>22</sup> Therefore, mPDT, which enables precise control of the number of PS administrations, has the potential to overcome the limitations of conventional single-dose PDT, which primarily affects the superficial tumor layers, and to extend therapeutic effects into deeper tumor regions.

This study confirmed the superiority of the therapeutic effect of red light compared to green light. In particular, the therapeutic effect of mPDT using the red OLED was shown to be expanded in both deep and horizontal directions with respect to the emitting surface. Red light penetrates deeper into tissue than does green light<sup>23</sup> and it allows a wider and more uniform distribution of light, including horizontally. Although the superiority of red light is known from conventional PDT studies,<sup>24</sup> the homogeneous illumination and fixed positioning of the light source contributed to the enhancement and expansion of the anti-tumor effect of red light, highlighting the advantages of the surface-emitting OLEDs.

Furthermore, the results of this study are supported by the emission spectrum of the OLED light source and the absorption characteristics of the photosensitizer. According to supplementary material Fig. 1(c), the integrated absorbance of temoporfin within the emission wavelength range of the red OLED (580–700 nm) is approximately three times higher than that within the emission range of the green OLED (500–630 nm). Moreover, since the emission intensities of the two light sources were set to be nearly identical in this study, it can be estimated that temoporfin absorbs approximately three times more light energy from the red OLED than from the green OLED. This suggests that the mPDT efficiency is higher with the red OLED.

## CONCLUSION

A new device has been constructed for the practical application of mPDT to tumors in deep organs. The thin, lightweight, and biocompatible OLED device is wirelessly powered and can illuminate entire tumors. Its effectiveness was proven in a rat hepatoma model by significantly reducing tumor size. This study is the first study to show that mPDT with a wirelessly powered, tumor-covering OLED device is effective for parenchymal organ cancers. The mPDT system could transform the treatment of deep organ cancers that are challenging to treat with conventional PDT. Future enhancements will include integration with an external, portable power unit to precisely control illumination timing, potentially revolutionizing cancer treatment and facilitating home-based care.



## METHODS

### Fabrication of the wirelessly driven OLED device

The layer configuration of an OLED element is as follows: transparent electrode/electron injection layer/electron transport layer/emission layer/hole transport layer/hole injection layer/aluminum.<sup>25</sup> Each layer was sequentially constructed on a polyethylene terephthalate substrate using a vacuum process. The fabricated structure was then exposed to ambient air and sealed with a sealing film. To this OLED element, a power-receiving coil, matching circuit unit, and ferrite sheet were added to form a wirelessly powered OLED device [Fig. 2(c)]. The power-receiving coil was constructed by etching copper foil formed on both sides of a polyimide substrate into a spiral pattern. The diameter of the coil was set at 13.6 mm, and two layers of coils with a wiring width of 0.2 mm and a number of turns of 7 were made to maximize resonance at 13.56 MHz most efficiently. The matching circuit and the use of ferrite sheets were tuned to optimize the Q-factor (supplementary material Table 1). After integration of the OLED element and receiver coil, they were coated with a UV-curable resin made of urethane polymer to wraparound the entire body.

### Parylene coating of the OLED device

Dichloro (2,2) paracyclophane monomer (Dix-C, PARYLENE JAPAN, Tokyo, Japan) was vaporized by heating to 150 °C under reduced pressure to 3.0 Pa using a chemical vapor deposition apparatus, a system of interconnected components (monomer vaporization chamber–heating furnace–deposition chamber) fabricated in our laboratory (K.F.). The vaporized monomer was then transferred to a chamber set at 680 °C and decomposed into monomeric diradicals. The monomers were reheated to 150 °C and vaporized again. This vapor was then diffused into a room-temperature chamber in which the OLED devices were placed. The monomers were polymerized, resulting in a thin film of poly (p-xylylene) derivative (Parylene C). After a 1- $\mu$ m-thick Parylene C film was accumulated, the OLED devices were rotated and coated with an additional 1- $\mu$ m-thick Parylene C film to minimize coating non-uniformity. By this method, the edges of the devices were also adequately coated.

### Fabrication of the wireless power transmission platform

The newly constructed wireless power transmission platform consists of a high-frequency power generator, a power amplifier (PT200A, Pleiades Technologies, Fukuoka, Japan), a power meter (SX200, DAI-ICHI DENPA KOGYO, Tokyo, Japan), and a container holding an antenna transmitting a 13.56 MHz radio wave (PTA-A3, Pleiades Technologies, Fukuoka, Japan) [Fig. 2(d)]. The container was box-shaped and its dimensions were configured to be 340 (W)  $\times$  500 (L)  $\times$  160 (H) mm (internal dimensions) and 440  $\times$  600  $\times$  170 mm (external dimensions), being sufficient to house a standard cage [bottom dimensions: 206 (W)  $\times$  365 (L) mm, uppermost dimensions: 263 (W)  $\times$  426 (L) mm, height: 202 mm] for multiple rats [Fig. 2(e)]. The transmission efficiency to the OLED device was measured to be 0.06% (supplementary material Fig. 5), likely due to the small size of the receiving coil relative to the transmitting coil.

### Orthotopic tumor model

Six-week-old male Sprague Dawley (SD) rats (186–202 g) (Japan SLC Inc., Japan) residing within the SPF area were used. To establish an orthotopic hepatoma model, SD rats were administered a compound anesthetic [medetomidine (0.3 mg/kg) (Nippon Zenyaku Kogyo, Japan), midazolam (4.0 mg/kg) (Sandz Corp., Japan), and butorphanol (5.0 mg/kg) (Meiji Seika Pharma, Japan)]. A minor laparotomy was performed, allowing the left lobe of the liver to be exposed, followed by an injection of 30  $\mu$ l of N1-S1 (A rat hepatoma cell line, ATCC, CRL-1604, Manassas, VA) cell suspension ( $2.0 \times 10^5$  cells) in phosphate-buffered saline into the subhepatic capsule with a 30 G needle (Fig. 3). Tumor size was gauged using an ultrasonic imaging system (10 MHz probe, VEVO770, VISUAL SONIC, Toronto, Ontario, Canada). Individual rats exhibiting tumor volumes between 20 and 30 mm<sup>3</sup>, as determined on the fourth-day post-implantation, were selected for inclusion in the experiments.

### Metronomic PDT in the orthotopic tumor model

After the tumor reached a certain size (20–30 mm<sup>3</sup>) (approximately 4 days after inoculation of cancer cells), mTHPC was administered via the tail vein (0.5 mg/kg). Subsequent to intraperitoneal administration of the compound anesthetic, laparotomy was performed to expose the left lobe of the liver. The location of the tumor was verified via an ultrasound system, and the OLED device was positioned so that the center of the tumor was aligned with the center of the OLED's emitting surface. Medical-grade cyanoacrylate adhesive (5  $\mu$ l) (Aron alpha A, Daiichi Sankyo, Japan) was applied to the OLED's four corners to secure the device affixed onto the liver (Fig. 3).

The rats were then transferred to a cage on the antenna board. Light emission was started 3 h after PS administration, coinciding with the peak of PS uptake in tumors,<sup>26</sup> and continued for 48 h. The transmitter power was set at 8 W for both green and red OLEDs. For the group with administration of the PS twice, an additional dose of mTHPC (0.5 mg/kg) was administered via the tail vein and light emission was continued for another 48 h. The second PS dose, the timing of which was based on the decrease in PS concentration in the tumors (supplementary material Fig. 8). After completion of mPDT, the tumor size was measured by an ultrasound imaging system and then the rats were euthanized and the left liver lobe of each rat was extracted.

### Photosensitizer (PS)

Temoporfin [5,10,15,20-tetrakis (3-hydroxyphenyl) chlorin; mTHPC] (SML1707, Sigma-Aldrich) was dissolved in anhydrous ethanol (443611, Sigma-Aldrich) and then in propylene glycol (3980039, Sigma-Aldrich) to make a 1 mg/ml solution (anhydrous ethanol:propylene glycol = 9:14). The solution was diluted fivefold with Milli-Q water and administered through the tail vein of each rat (0.5 mg/kg).

For the measurement of absorbance spectra of the PS, a 0.2-mg/ml aqueous solution of mTHPC was prepared, and the absorbance was measured using a spectrophotometer (JASCOV630; Shimadzu Corporation, Tokyo, Japan).

### Additional methods

Other experimental methods are described in detail in the supplementary material and additional methods.

## SUPPLEMENTARY MATERIAL

See the [supplementary material](#) for the following:

- Additional methods
- Optimizing energy transmission with a resonant coil and electromagnetic shielding ([supplementary material](#) Table 1)
- Enhanced luminescence uniformity and photosensitizer compatibility in OLED systems for efficient photodynamic reaction ([supplementary material](#) Fig. 1)
- Durable water-sealed OLED devices for continuous in-body light emission and long-term implantation ([supplementary material](#) Fig. 2)
- Mitigating foreign body reactions in implantable OLED devices using Parylene C coating. Minimal heat generation and absence of thermal damage in *in vivo* OLED device applications ([supplementary material](#) Fig. 3)
- Stable power transmission system for uniform OLED activation in freely moving rodents ([supplementary material](#) Fig. 4)
- Evaluation of wireless power transmission efficiency for an implanted OLED device in a rat model ([supplementary material](#) Fig. 5)
- Estimation of total light energy delivered to tumors during mPDT using OLED devices ([supplementary material](#) Fig. 6)
- Evaluation of mPDT-induced effects on normal liver tissue and body weight ([supplementary material](#) Fig. 7)
- Optimizing mPDT efficacy through timing and redistribution of photosensitizers ([supplementary material](#) Fig. 8)
- [Supplementary material](#) Video 1, [supplementary material](#) Video 2, and References

## ACKNOWLEDGMENTS

We thank K. Aoki and Y. Mitsui for their technical assistance; Dr. T. Fujie (Tokyo Institute of Technology, Japan) and Dr. K. Yamagishi (SUTD, Singapore) for discussions; and the staff of the R&D Dept. of MORESCO Corporation (Kobe Japan) for providing sealing resin. Y. Mo. is supported by the JSPS KAKENHI Grant (21H03846 and 21K19935), the Fukuda Foundation for Medical Technology, The Uehara Memorial Foundation, the Suzuken Memorial Foundation, and the Takeda Science Foundation. K.F. is supported by the JST A-Step Grant (JPMJTM20GY), the Kyutec Research Grant, and the Tateishi Science and Technology Foundation (B2221904). K.M. is supported by JSPS KAKENHI Grant (19H02599).

## AUTHOR DECLARATIONS

### Conflict of Interest

The authors have no conflicts to disclose.

### Ethics Approval

Ethics approval for experiments reported in the submitted manuscript on animal or human subjects was granted. All animal protocols were approved by the National Defense Medical College Animal Care and Use Committee (Approval Nos. 19009 and 23045).

## Author Contributions

**Yujiro Itazaki:** Conceptualization (equal); Data curation (lead); Investigation (lead); Methodology (lead); Writing – original draft (lead); Writing – review & editing (equal). **Kei Sakanoue:**

Conceptualization (equal); Investigation (equal); Methodology (equal); Supervision (equal); Writing – review & editing (equal). **Katsuhiko Fujita:** Conceptualization (equal); Funding acquisition (equal); Investigation (equal); Methodology (equal); Supervision (equal); Writing – review & editing (equal). **Izumi Kirino:** Investigation (equal). **Kazuhiro Eguchi:** Investigation (equal). **Yutaka Miyazono:** Investigation (equal). **Ryoichi Yamaguchi:** Investigation (equal). **Takasumi Tsunenari:** Investigation (equal). **Takao Sugihara:** Investigation (equal). **Kenji Kuwada:** Investigation (equal). **Naoki Kobayashi:** Investigation (equal). **Tsuyoshi Goya:** Investigation (equal). **Katsuyuki Morii:** Funding acquisition (equal); Investigation (equal). **Hironori Tsujimoto:** Supervision (equal). **Yuji Morimoto:** Conceptualization (lead); Funding acquisition (equal); Methodology (supporting); Supervision (lead); Writing – original draft (equal); Writing – review & editing (lead).

## DATA AVAILABILITY

The data that support the findings of this study are available from the corresponding author upon reasonable request.

## REFERENCES

- <sup>1</sup>D. E. Dolmans, D. Fukumura, and R. K. Jain, “Photodynamic therapy for cancer,” *Nat. Rev. Cancer* **3**(5), 380–387 (2003).
- <sup>2</sup>S. K. Bisland, L. Lilge, A. Lin, R. Rusnov, and B. C. Wilson, “Metronomic photodynamic therapy as a new paradigm for photodynamic therapy: Rationale and preclinical evaluation of technical feasibility for treating malignant brain tumors,” *Photochem. Photobiol.* **80**, 22–30 (2004).
- <sup>3</sup>A. Bansal, F. Yang, T. Xi, Y. Zhang, and J. S. Ho, “In vivo wireless photonic photodynamic therapy,” *Proc. Natl. Acad. Sci. U. S. A.* **115**(7), 1469–1474 (2018).
- <sup>4</sup>K. Yamagishi, I. Kirino, I. Takahashi, H. Amano, S. Takeoka, Y. Morimoto, and T. Fujie, “Tissue-adhesive wirelessly powered optoelectronic device for metronomic photodynamic cancer therapy,” *Nat. Biomed. Eng.* **3**(1), 27–36 (2018).
- <sup>5</sup>I. Kirino, K. Fujita, K. Sakanoue, R. Sugita, K. Yamagishi, S. Takeoka, T. Fujie, S. Uemoto, and Y. Morimoto, “Metronomic photodynamic therapy using an implantable LED device and orally administered 5-aminolevulinic acid,” *Sci. Rep.* **10**(1), 22017 (2020).
- <sup>6</sup>S. B. Brown, E. A. Brown, and I. Walker, “The present and future role of photodynamic therapy in cancer treatment,” *Lancet Oncol.* **5**(8), 497–508 (2004).
- <sup>7</sup>M. Seshadri, D. A. Bellnier, L. A. Vaughan, J. A. Sperry, R. Mazurchuk, T. H. Foster, and B. W. Henderson, “Light delivery over extended time periods enhances the effectiveness of photodynamic therapy,” *Clin. Cancer Res.* **14**(9), 2796–2805 (2008).
- <sup>8</sup>D. Nowis, T. Stoklosa, M. Legat, T. Issat, M. Jakobisiak, and J. Golab, “The influence of photodynamic therapy on the immune response,” *Photodyn. Ther.* **2**(4), 283–298 (2005).
- <sup>9</sup>J. F. Algorri, M. Ochoa, P. Roldan-Varona, L. Rodriguez-Cobo, and J. M. Lopez-Higuera, “Light technology for efficient and effective photodynamic therapy: A critical review,” *Cancers* **13**(14), 3484 (2021).
- <sup>10</sup>R. Bonnett, R. D. White, U. J. Winfield, and M. C. Berenbaum, “Hydroporphyrins of the meso-tetra(hydroxyphenyl)porphyrin series as tumour photosensitizers,” *Biochem. J.* **261**(1), 277–280 (1989).
- <sup>11</sup>G. Gunaydin, M. E. Gedik, and S. Ayan, “Photodynamic therapy—Current limitations and novel approaches,” *Front. Chem.* **9**, 691697 (2021).
- <sup>12</sup>S. M. Thompson, M. R. Callstrom, B. Knudsen, J. L. Anderson, R. E. Carter, J. P. Grande, L. R. Roberts, and D. A. Woodrum, “Development and preliminary testing of a translational model of hepatocellular carcinoma for MR imaging and interventional oncologic investigations,” *J. Vasc. Interventional Radiol.* **23**(3), 385–395 (2012).
- <sup>13</sup>C. A. Morton, C. Whitehurst, J. V. Moore, and R. M. Mackie, “Comparison of red and green light in the treatment of Bowen’s disease by photodynamic therapy,” *Br. J. Dermatol.* **143**(4), 767–772 (2000).



- <sup>14</sup>G. Laimer, P. Schullian, N. Jaschke, D. Putzer, G. Eberle, A. Alzaga, B. Odisio, and R. Bale, "Minimal ablative margin (MAM) assessment with image fusion: An independent predictor for local tumor progression in hepatocellular carcinoma after stereotactic radiofrequency ablation," *Eur. Radiol.* **30**(5), 2463–2472 (2020).
- <sup>15</sup>I. Joo, K. W. Morrow, S. S. Raman, J. P. McWilliams, J. W. Sayre, and D. S. Lu, "CT-monitored minimal ablative margin control in single-session microwave ablation of liver tumors: An effective strategy for local tumor control," *Eur. Radiol.* **32**(9), 6327–6335 (2022).
- <sup>16</sup>J. Y. Choi, J. M. Lee, and C. B. Sirlin, "CT and MR imaging diagnosis and staging of hepatocellular carcinoma: Part I. Development, growth, and spread: Key pathologic and imaging aspects," *Radiology* **272**(3), 635–654 (2014).
- <sup>17</sup>M. Golda-Cepa, K. Engvall, M. Hakkarainen, and A. Kotarba, "Recent progress on parylene C polymer for biomedical applications: A review," *Prog. Org. Coat.* **140**, 105493 (2020).
- <sup>18</sup>B. D. Winslow, M. B. Christensen, W.-K. Yang, F. Solzbacher, and P. A. Tresco, "A comparison of the tissue response to chronically implanted Parylene-C-coated and uncoated planar silicon microelectrode arrays in rat cortex," *Biomaterials* **31**(35), 9163–9172 (2010).
- <sup>19</sup>H. S. Lim, "Reduction of thermal damage in photodynamic therapy by laser irradiation techniques," *J. Biomed. Opt.* **17**(12), 128001 (2012).
- <sup>20</sup>G. Shafirstein, D. A. Bellnier, E. Oakley, S. Hamilton, M. Habitzruther, L. Tworek, A. Hutson, J. A. Sperryak, S. Sexton, L. Curtin, S. G. Turowski, H. Arshad, and B. Henderson, "Irradiance controls photodynamic efficacy and tissue heating in experimental tumours: Implication for interstitial PDT of locally advanced cancer," *Br. J. Cancer* **119**(10), 1191–1199 (2018).
- <sup>21</sup>M. D. Savellano, N. Owusu-Brckett, J. Son, T. Ganga, N. L. Leung, and D. H. Savellano, "Photodynamic tumor eradication with a novel targetable photosensitizer: Strong vascular effects and dependence on treatment repetition versus potentiation," *Photochem. Photobiol.* **89**(3), 687–697 (2013).
- <sup>22</sup>M. Korbek and M. R. Hamblin, "The impact of macrophage-cancer cell interaction on the efficacy of photodynamic therapy," *Photochem. Photobiol. Sci.* **14**(8), 1403–1409 (2015).
- <sup>23</sup>T. J. Pfefer, L. S. Matchette, C. L. Bennett, J. A. Gall, J. N. Wilke, A. J. Durkin, and M. N. Ediger, "Reflectance-based determination of optical properties in highly attenuating tissue," *J. Biomed. Opt.* **8**(2), 206–215 (2003).
- <sup>24</sup>K. M. M. Rahman, S. Kumbham, G. Bist, S. Woo, B. A. Foster, and Y. You, "Comparison of red and green light for treating non-muscle invasive bladder cancer in rats using singlet oxygen-cleavable prodrugs with PPIX-PDT," *Photochem. Photobiol.* **100**(6), 1659–1675 (2024).
- <sup>25</sup>H. Fukagawa, K. Suzuki, H. Ito, K. Inagaki, T. Sasaki, T. Oono, M. Hasegawa, K. Morii, and T. Shimizu, "Understanding coordination reaction for producing stable electrode with various low work functions," *Nat. Commun.* **11**(1), 3700 (2020).
- <sup>26</sup>P. Cramers, M. Ruevekamp, H. Oppelaar, O. Dalesio, P. Baas, and F. A. Stewart, "Foscan<sup>®</sup> uptake and tissue distribution in relation to photodynamic efficacy," *Br. J. Cancer* **88**(2), 283–290 (2003).